Design, Analysis and Comparison of Various MEMS Switches for Reconfigurable Planar Antenna

Paras Chawla[1*], Rajesh Khanna[2]

[1*]Electronics & Communication Engineering, JMIT, Radaur, Kurukshetra University, Haryana (India)-135133, paras.chawla@jmit.ac.in

[2]Department of Electronics & Communication Engineering Thapar University, Patiala, Punjab-147004, India, rkhanna@thapar.edu

Abstract: This paper presents design and analysis of a novel beam for electrostatically actuated Radio Frequency Micro Electro Mechanical Systems (RF MEMS) shunt switches. In the proposed beam design, geometrical variations in terms of structure shape, material, gap, introduction of holes and changing the length and width of anchor have led to good RF performance. The holes in the beam (maximum up to 60% of total area of upper electrode) not only make the smooth mechanical movement of the beam but also result in low spring constant. The designed RF-MEMS switches are actuated electrostatically, and can be operated at low pull-in voltage, ranging from 0.5 V to 22 V with negligible power consumption. Proposed RF MEMS switches can easily be integrated in mobile RF front end section alongwith microstrip antenna in order to provide reconfigurabilty in frequency. Various shapes of planar antenna are also discussed which are suitable with proposed shunt switches. The effect of microstrip line and coplanar waveguide as transmission line are also studied.

Keywords: Electromagnetics; Finite element methods; Microelectromechanical systems; PolyMUMPS; Optimization

1 Introduction

The fabrication of integrated MEMS device for RF circuits design has a key impact on small-sized reconfigurable antennas [1, 2, 3]. In the present age, microelectronic switching take up a important position in make sure reconfigurability for frequency tuning, beam steering and its shaping. Recently, MEMS on/off switches have shown very good RF characteristics, including smaller size, lower insertion loss in on state, almost zero power consumption, higher isolation in off state, extreme lower intermodulation distortion and weight [4, 5, 29]. The switch's capability to achieve well upto 50 GHz is a noteworthy leap forward over solid-state and mechanical RF switches [6, 30]. The RF MEMS

switches are applied on various shapes and geometry of microstrip antennas like planar inverted F-shape (PIFA), E-shape, S-shape, spiral, fractal and many more to achieve different applications. The fractal antenna has feature of self-similar shapes and can also provide the reason for the design of multi band frequency antennas [7]. There are numerous fractal geometries like sierpinski carpet, sierpinski gasket, hilbert curve, koch island, and minkowski etc which have been used in fractal antennas [7]. Sierpinski gasket is the main predecessor which is very widely studied. Various beam shapes and materials of capacitive MEMS RF switches prepared out of chromium, nickel, tantalum [19], tungsten, aluminum, copper, and gold have so far been presented in previous work for beam design [11-27]. The essential for low pull-in voltage in MEMS RF switches has often produced excessive fabrication complication as well as extent of the device. PolyMUMPs has followed the idea of standard process steps approach as a much clear path to device functionality and volume production [8]. For larger scale systems, PolyMUMPs chips act as a standard building unit, where the microelectromechanical chip is only single piece of the overall building block. PolyMUMPs technology is also used as a benchmarking tool for statistical studies and software models, where experimented and measured data from actually fabricated chips are validated with theories [8, 9]. The key emphasis in this work is the study and designing of improved beams for RF MEMS shunt switches which seems compatible with multiband microstrip antennas.

2 Principles and Operation of MEMS RF Switch

MEMS designs are the combination of sensors, mechanical elements, electronics and actuators part on a semiconductor wafer through surface and bulk micro-fabrication process. This process generally involves a photo-lithography typed micro-machining, batch production base fabrication, which usually offers benefits of lowest cost while producing in huge volume [26, 27]. MEMS RF switches can be air bridge, or a diaphragm, thin metal conducting cantilever can be considered from point of mechanics. From radio frequency circuit configuration, it can be parallel coupled or series coupled with an t-line [10]. The physical connection can be either resistive i.e. metal-to-metal or capacitive i.e. metal–insulator–metal type. Each such configuration of switch RF has many advantages in terms of manufacturability or working performance.

When the external pull-in is applied on the actuation pad, an electrostatic power is generated on the switch beam [28, 32, 34]. The reaction force (F) balance the generated electrostatic force produced in beam structure. At two-third air gap, the switch beam becomes unstable and results in breakdown at the lower transmission line in down-state position [29-34]. The pull-in voltage be influenced by the value spring constant of beam shape, gap and electrode area [1, 28]. In this research we have proposed various beam shape designs to lesser the k value.

Calculation of k for meander formed Serpentine flexure beam [5] is specified as under-

$$k \approx \frac{48GJ}{l_a^2\left(\frac{GJ}{EI_x}l_a + l_b\right)n^3} \qquad \text{for} \qquad n >> \frac{3l_b}{\frac{GJ}{EI_x}l_a + l_b} \tag{1}$$

where n is the amount of meanders used in the serpentine beam flexure,

$G = {}^{E}/_{2(1+v)}$ represent torsion modulus, $I_x = {}^{wt^3}/_{12}$ denotes moment of inertia. Further l_a, l_b and w are primary length, secondary length and width of the meander, E is the elasticity, v belongs to Poisson's ratio and the torsion constant is specified by,

$$J = \frac{1}{3}t^3 w\left(1 - \frac{192}{\Pi^5}\frac{t}{w}\sum_{i=1,odd}^{\infty}\frac{1}{i^5}\tanh\left(\frac{i\Pi w}{2t}\right)\right) \tag{2}$$

For the situation where $l_a \gg l_b$, the k of the serpentine beam flexure turn into

$$k \approx 4Ew\left({}^{t}/_{(nl_a)^3}\right) \tag{3}$$

2.1 Design of Transmission Lines

Coplanar waveguide (CPW) is a three-conductor on one-sided t-line. CPW has center conductor alongwith two grounds lying in same plane, reducing the effects of coupling and allowing for easy addition of shunt and series elements. Since microwave ICs are basically coplanar in construction and therefore CPW lines are used commonly as circuit parts and be integrated lines. At mm-wave frequencies, CPW deals the prospective of lesser conductor and radiation losses as related to microstrip lines. CPW has important advantage of varying magnitudes of the t-line without effecting the value of characteristic impedance [6, 10, 28].

An estimated formula [10], for the typical impedance of the CPW, assuming t is very small, 0 < k < 1, and h >> w, is

$$Z_o = \frac{30\pi^2}{\sqrt{(\varepsilon_r + 1)/2}}[\ln(2\frac{1+\sqrt{p}}{1-\sqrt{p}})]^{-1}\,\text{ohms} \tag{4}$$

$$p = \frac{w}{w+2s} \tag{5}$$

where w is center strip width, s is slot width, and ε_{re} is relative dielectric constant of the material.

An empirical calculation for effective ε_{re} [10] is mention as-

$$\varepsilon_{re} = \frac{\varepsilon_r + 1}{2}\left[\tanh\left(1.785\log\left(\frac{h}{w} + 1.75\right) + \frac{pw}{h}\left(0.04 - 0.7p + (1 - 0.1\varepsilon_r)\frac{(0.25 + p)}{100}\right)\right)\right] \tag{6}$$

Further, microstrip transmission may be considered as a two wire line and is further viewed the most extensively used as a planar microstrip transmission line [29-31]. One side of the design is free to access for mounting on the hymite or other packaged devices and further geometrical construction lends itself well to printed circuit board patterning methods to define the complete circuit. Planar transmission line has been used extensively in microwave and millimeter circuits and systems.

The structure is complex and due to which the mathematical expression of per unit length dimensions is difficult to calculate. The approximated analytical expression of effective relative permittivity is given as

$$\frac{1}{2}\frac{\in_0 WwV^2}{g^2} = p(g_0 - g) \tag{7}$$

where, g – separation between upper and bottom electrode and g_o – relaxed gap. Microwave post-parameters which ought to be optimized for MEMS switch are the return loss, isolation, insertion loss (IL) and switching operating frequency. The IL is due to misalliance of the impedance of t-line and RF switch. The contact beam resistance and metallization loss will also added to the IL. RF MEMS influence on above mentioned microwave post-parameters results will be included in preceeding sections.

3 Switch Design and Simulation Results

We have proposed four different beam structures designs, whose micro fabrication steps are explained by using the modeling action involved in the designing of MEMS switches. A thorough modeling and analysis of all four designed switches has been offered based on multi-physics coventorware software, take out their key performance characteristics and the results are intuitionistic. We have also used this software to recognize the relationship between shape, material and actuated voltage of RF switch. Further, variation of displacement in switch i.e. from maximum z-direction to minimum z-direction w.r.t. voltage is shown, when the switch is electrostatically actuated.

3.1 Modeling Action of Various RF MEMS Switch

Table 1 shows the processed file of design-1 RF switch. The switch is designed on silicon substrate of dimension 280×150 μm^2, relative dielectric constant 11.9, and thickness 10 µm which is covered with silicon nitrate of thickness 0.2 µm. The microstrip transmission line are made up of titanium (Ti) of thickness 0.5 µm and complete geometry with dimension and equivalent circuit (in down state) is shown in Figure 1(a-c). Holes are used, in three out of four designed switches, in upper beam electrode to increase the switching mechanism, reduce the squeeze film damping and lowering the mass of beam. The electrostatic actuation can be decreased using: reduction in the spring constant of beam, minimize the air gap, and increase the actuation area.

Table 1
Process file of design-1 capacitive switch

Sr. No.	Step Name	Layer Name	Material Name	Thickness (µm)	Mask Name	Photoresist
1.	Substrate	Substrate	Silicon (100)	10	Ground	
2.	Stack Material	Nitride	Silicon Nitride (SIN)	0.2		
3.	Planar Fill	Waveguide	Titanium	0.5		
4.	Straight Cut				Waveguide	+
5.	Planar Fill	Sacrifical	BPSG	1.0		
6.	Straight Cut				Anchor	-
7.	Conformal Shell	Beam	Gold	0.5		
8.	Straight Cut				Beam	+
9.	Straight Cut				Holes	-
10.	Sacrifice		BPSG			

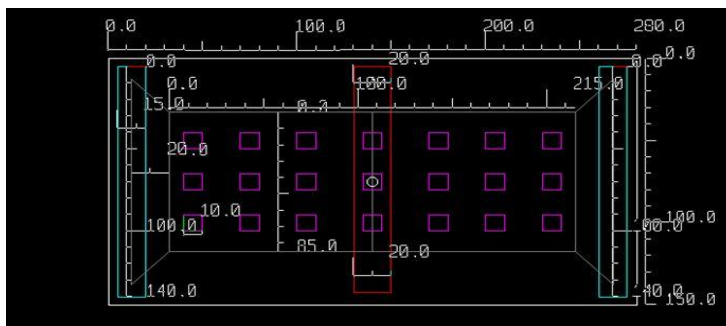

(a)

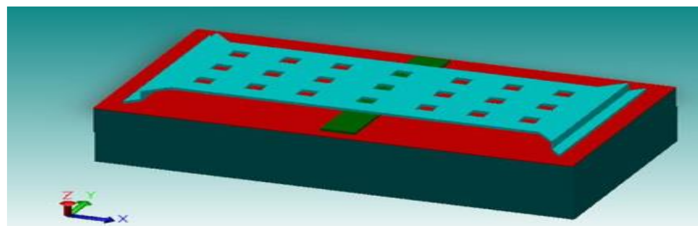

(b)

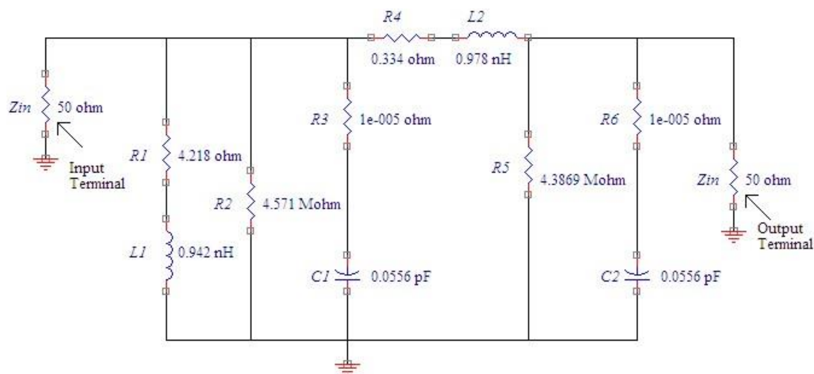

(c)

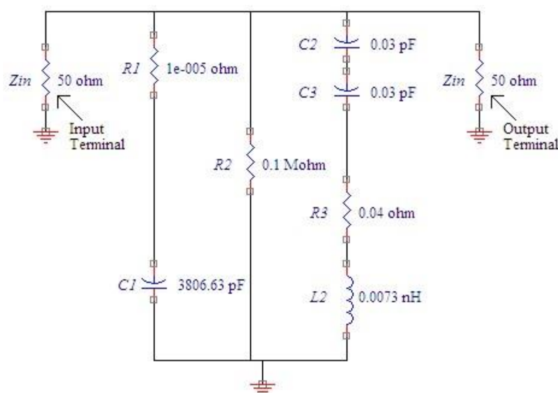

(d)

Figure 1
(a) 2-D layout with dimension of beam (b) 3-D layout of 'Design-1' capacitive switch. Equivalent circuit of Design-1 in (c) up position and (d) down position.

The equivalent model of shunt MEMS switch is used to find the *L, R* and *C* parameters, where *L* is the inductance, *R* is the beam resistance and *C* is the capacitance of bridge in up and down state. In this work, the actual circuit of proposed "Design-1" structure of Fig. 1(b) is generated by means of HSPICE

model file. The HSPICE file from HFSS solver is exported in Advanced Design System (ADS) software to validate the results through circuit and layout approach. The equivalent model shown in Fig. 1 (c) and 1 (d), the bridge is represented by the two short segments of transmission line and a lumped LCR model of the bridge having a different up- and down-position capacitance value [1]. The bridge capacitance in down state is due to the bridge-dielectric and transmission line active overlapping area. Further, up-state is due to the active overlapping area between the beam and the conductor. The up-state capacitance (C_{up}) is always less than the down-state capacitance (C_{down}). This effect is due to the collapse of MEMS upper electrode/bridge on the dielectric surface, when an electrostatic actuation is applied between the transmission line and the switch bridge. The equivalent generated electrostatic force causes the largely increase in the switch beam capacitance. The LCR model of shunt capacitive MEMS switch obeys the rules as an inductor above the series resonant frequency, as a capacitor below this frequency and decreases as a series resistance at resonance. Further, in up-position of switch, the inductance plays no role and only shunt capacitance has a major role to define/model the MEMS bridge. Although, it is observed in down-position of the MEMS bridge, the inductance plays a significant role [1].

For design-1 MEMS switch analysis, the resonant frequency occurs at 22 GHz for C_{up} = 0.0556 pF and L_{up} = 0.942 nH, when it is in on-position. For C_{down} = 3806.63 pF and L_{down} = 0.0073 nH, the switch resonate at 1 GHz frequency when the MEMS bridge is in down or off position. According to these circuit values, the insertion loss measured 0.34 dB at 4 GHz and 0.98 dB at 8 GHz in on-condition. The values of isolation are 67.6 dB at 4 GHz and 73.6 dB at 8 GHz in off-condition. The electromagnetics parameters are optimized by varying the shunt inductance and capacitance values. Except the characteristics impedance (Z_0 = 50 ohm), other circuit values are permitted to vary the isolation and insertion loss results calculations. It has been observed that by decreasing the C_{up} from 0.0556 pF to 55.6 fF and by increasing L_{up} from 0.942 nH to 29.42 nH, the insertion value improves and value 0.22 dB at 4 GHz and 0.61 dB at 8 GHz, respectively. Similarly, in down position the optimized isolation has been achieved 87.68 at 4 GHz and 93.59 dB at 8 GHz, by increasing L_{down} from 0.0073 nH to 73 pH and at the same time by increasing C_{down} from 3806.63 pF to 38.06 nF. For these optimized circuit elements, the switch resonates at 3.94 GHz and 0.95 GHz in on- and off-condition, respectively.

The DC-contact shunt design-2 and design-3 switches designing steps are same in up-position as that of design-1 except that the silicon nitride film is removed below the metal bridge. As a result, there is a contact of metal to metal layer among the transmission line and the ground surface. In the down-position of these two DC contact shunt MEMS switches results in an $R_{Sh}L_{down}$ equivalent circuit-model in parallel with the transmission line. Shunt resistance (R_{Sh}) is the addition of the metal bridge resistance and the contact resistance. The LRC parameters extraction of both switches follows the same method as the design-1 capacitive

shunt MEMS switch. The design-2 up-state results show that by increasing inductance from 0.352nH to 3.5 nH, the insertion loss 0.378 dB at 4 GHz and 0.10 dB at 8 GHz can be achieved. The isolation value in the down-state of design-2 switch can be optimized up to 45.9 dB at 4 GHz and 45.8 dB at 8 GHz by decreasing the shunt inductance from 0.0123 nH to 12.3 pH. Similar statement has been observed for design-3 switch. The optimized results of insertion loss (0.36 dB at 4 GHz and 0.096 at 8 GHz) and isolation (39.6 dB at 4 GHz and 39.6 dB at 8 GHz) can be achieved by selecting L_{up} equal to 3.57 nH and L_{down} equal to 0.122 pH, respectively. Further, the simulated up state capacitance and isolation results are verified from following equations [1],

$$|S_{11}|^2 \cong \frac{w^2 C_{up}^2 Z_o^2}{4} \tag{8}$$

and

$$|S_{21}|^2 \cong \begin{cases} \left(\frac{2R_s}{Z_o}\right)^2 & for\ wL \ll R_s \\ \left(\frac{2\sqrt{2}R_s}{Z_o}\right)^2 & for\ wL = R_s \\ \left(\frac{2wL}{Z_o}\right)^2 & for\ wL \gg R_s \end{cases} \tag{9}$$

Finally, the design-4 capacitive shunt MEMS switch results show optimized insertion loss i.e. 0.051 dB at 4 GHz and 0.198 dB at 8 GHz, when L_{up} is equal to 0.0542 nH and C_{up} is equal to 76.8 fF. In the down position, the optimized isolation i.e. 22.41 dB at 4 GHz and 22.66 dB at 8 GHz can be achieved by selecting circuit component values as L_{down} equal to 0.023 nH and C_{down} equal to 8.12 pF, respectively.

Figure 2 show the 2D layout with dimensions of other three designed MEMS shunt RF switches. The equivalent circuit of design-2 DC shunt MEMS switch is shown in Figure 3.

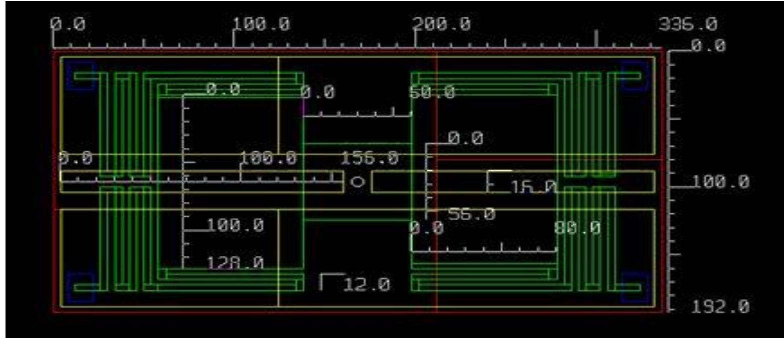

(a)

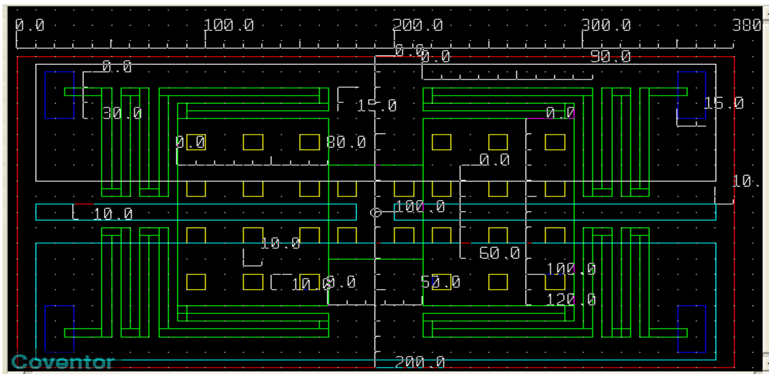

(b)

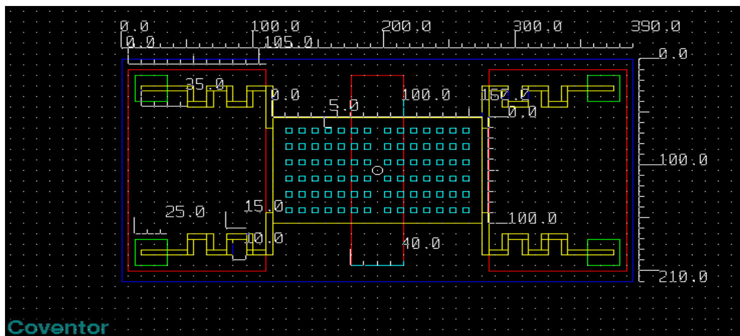

(c)

Figure 2

(a) 2-D layout with dimension of 'Design-2' (b) 2-D layout with dimension of 'Design-3' (c) 2-D layout with dimension of 'Design-4' switch

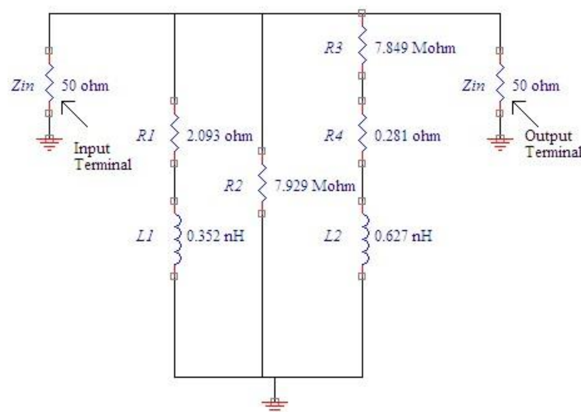

(a)

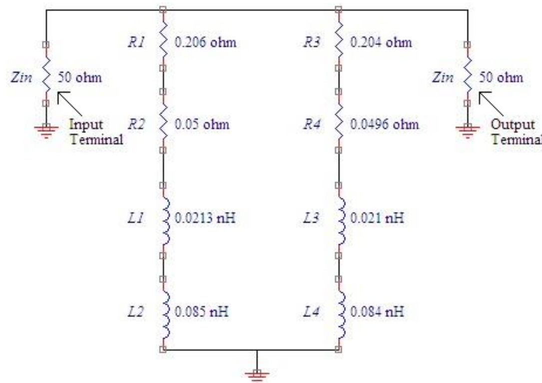

(b)

Figure 3
Equivalent circuit of Design-2 MEMS shunt switch in (a) up position and (b) down position

3.2 Analysis of Various RF MEMS Switches – Multiphyics Properties

After designing various RF MEMS switches are analysed. The voltage versus charge has been shown for various beam structures in Table 2. The voltage on beam is applied 1V w.r.t. ground in each case. The charge values on various beams are 0.185 pC, 0.355 pC, 0.354 pC & 0.311 pC, respectively. Further the Tables 3 to 6 show the capacitance matrix of various beam structures of switches. The development of multilayer design and accumulation of a metal layer into the process permitted a unlimited increase of the MEMS switch on-position capacitances. By introduction of the metal layer, prominent to a C_{on}/C_{off} ratio higher which is at maximum 50 times more than the ones attained without this feature [4]. Maximum and minimum displacement of various switches in X, Y, Z directions are shown in Table 7. The reaction forces in three directions of various designed switches have been shown in Table 8. The reaction forces that developed at the fixed ends is a result of pressure load is exerted in downward direction. The occurrence of natural vibration at some specific frequencies results the existence of modal shapes. Such vibrating response assumes the properties of physical system. At equilibrium, the resonant frequencies of MEMS upper electrode is calculated. The different mode shapes and their concern frequencies are very much resembles the characteristics of under-damped response.

Table 2
Charge values of all four designed switches at beam voltage = 1V

	Charge value (pC)
Design-1	1.85×10^{-1}
Design-2	3.55×10^{-1}
Design-3	3.54×10^{-1}
Design-4	3.11×10^{-1}

Table 3
Capacitance matrix (pF) of 'Design-1' switch

	Ground	CPW	Beam
Ground	2.933×10^{-1}	-1.226×10^{-1}	-1.707×10^{-1}
CPW	-1.226×10^{-1}	1.373×10^{-1}	-1.466×10^{-2}
Beam	-1.707×10^{-1}	-1.466×10^{-2}	1.853×10^{-1}

The MEMS beam switch response should be prefered below the mode 1 resonant frequency in order to avoid peak in displacement. So, the prime objective is always increase the performance of switch upper beam structure first mode resonance frequency. Figure-3 show the harmonic analysis and the modes of design-1 switch.

Table 4
Capacitance matrix (pF) of 'Design-2' switch

	Ground	Wgnd1	Wcon1	Wgnd2	Wcon2	Beam
Ground	2.265	-1.015	-9.926×10^{-2}	-1.014×10^{-1}	-9.925×10^{-1}	-3.705×10^{-2}
Wgnd1	-1.015	1.161	-6.908×10^{-5}	-2.707×10^{-5}	-9.193×10^{-5}	-1.457×10^{-1}
Wcon1	-9.926×10^{-2}	-6.908×10^{-5}	1.126×10^{-1}	-1.076×10^{-4}	-4.404×10^{-7}	-1.319×10^{-2}
Wgnd2	-1.014×10^{-1}	-2.707×10^{-5}	-1.076×10^{-4}	1.160	-9.458×10^{-5}	-1.456×10^{-1}
Wcon2	-9.925×10^{-1}	-9.193×10^{-5}	-4.404×10^{-7}	-8.458×10^{-5}	1.126×10^{-1}	-1.319×10^{-2}
Beam	3.705×10^{-2}	-1.457×10^{-1}	-1.319×10^{-2}	-1.456×10^{-1}	-1.319×10^{-2}	3.547×10^{-1}

Table 5
Capacitance matrix (pF) of 'Design-3' switch

	Ground	Wgnd1	Wcon1	Wgnd2	Wcon2	Beam
Ground	2.264	-1.015	-9.874×10^{-2}	-1.014	-9.873×10^{-2}	-3.770×10^{-2}
Wgnd1	-1.015	1.161	-6.908×10^{-5}	-2.707×10^{-5}	-9.193×10^{-5}	-1.457×10^{-1}
Wcon1	-9.874×10^{-2}	7.514×10^{-5}	1.121×10^{-1}	-1.219×10^{-4}	-7.423×10^{-7}	-1.324×10^{-2}
Wgnd2	-1.014	-2.806×10^{-5}	-1.219×10^{-4}	1.159	-9.832×10^{-5}	-1.449×10^{-1}
Wcon2	-9.873×10^{-2}	-9.832×10^{-5}	-7.423×10^{-7}	-9.842×10^{-5}	1.121×10^{-1}	-1.325×10^{-2}
Beam	-3.770×10^{-2}	-1.450×10^{-1}	-1.324×10^{-2}	-1.449×10^{-1}	-1.325×10^{-2}	3.542×10^{-1}

Table 6
Capacitance matrix (pF) of 'Design-4' switch

	Ground	Beam	Wgnd1	Wgnd2	Conductor
Ground	1.979	-7.739×10^{-2}	-8.110×10^{-1}	-8.109×10^{-1}	-2.801×10^{-1}
Beam	-7.739×10^{-2}	3.110×10^{-1}	-9.949×10^{-2}	-1.017×10^{-1}	-3.233×10^{-2}
Wgnd1	-8.110×10^{-1}	9.949×10^{-2}	9.106×10^{-1}	-8.968×10^{-5}	-2.933×10^{-5}
Wgnd2	-8.109×10^{-1}	-1.017×10^{-1}	-8.968×10^{-5}	9.128×10^{-1}	-2.931×10^{-5}
Conductor	-2.801×10^{-1}	-3.233×10^{-2}	-2.933×10^{-5}	-2.931×10^{-5}	3.125×10^{-1}

Table 7
Maximum & minimum displacement (in µm) of vector components of all designed switches

	Design-1		Design-2		Design-3		Design-4	
	Max	Min	Max	Min	Max	Min	Max	Min
Node Displacement	1.881	0	1.011	0	9.876×10^{-1}	0	1.666×10^{-1}	0
Node X Displacement	9.445×10^{-3}	-9.530×10^{-3}	4.221	-4.221	3.974	-3.974	4.40	-4.40×10^{-1}
Node Y Displacement	2.335×10^{-3}	2.241×10^{-3}	3.682	-3.682	3.509	-3.509	6.859×10^{-1}	-6.859×10^{-1}
Node Z Displacement	1.017×10^{-3}	-1.881	1.399×10^{-1}	-1.011×10^{-2}	1.356×10^{-1}	-9.876×10^{-1}	2.806×10^{-3}	-1.666×10^{-1}

Table 8
Vector components of force (in N/m^2) on various parts of all designed switches

	Design-1			Design-2			Design-3			Design-4		
	F_x	F_y	F_z	F_x	F_y	F_z	F_x	F_y	F_z	F_x	F_y	F_z
Anchor 1	2.219×10^{-1}	2.585×10^{-1}	9.358	5.567	2.225	7.668	-5.593	2.236	7.861	-2.556×10^{1}	5.611	4.337
Anchor 2	-2.219×10^{2}	-2.590×10^{-1}	9.363	5.567	-2.225	7.668	-5.593	-2.236	7.861	-2.556×10^{1}	-5.611	4.337
Anchor 3	-	-	-	-5.567	2.225	7.668	5.593	-2.236	7.861	2.556×10^{1}	5.611	4.337
Anchor 4	-	-	-	-5.567	-2.225	7.668	5.593	2.236	7.861	2.556×10^{1}	-5.611	4.337

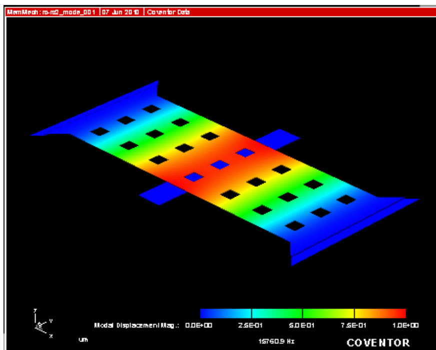

(a)

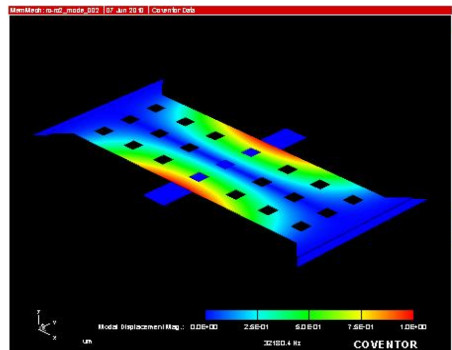

(b)

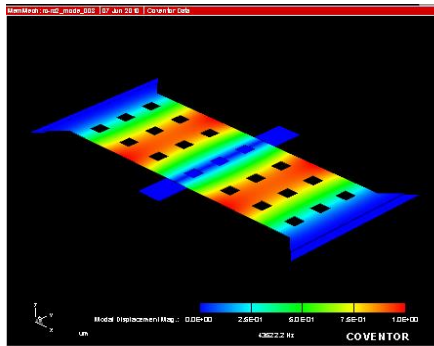

(c)

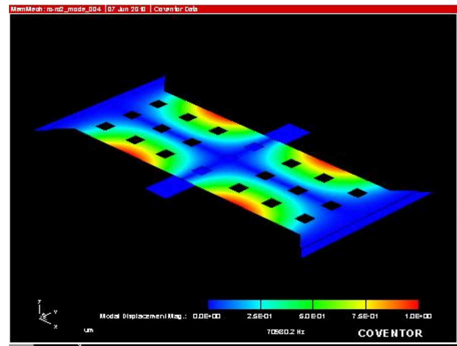

(d)

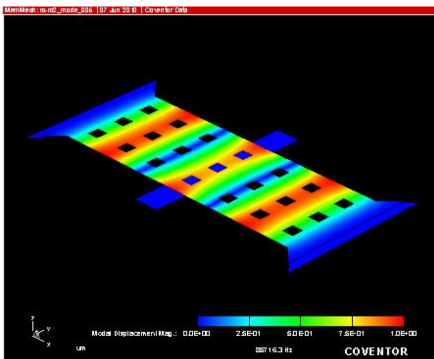

(e)

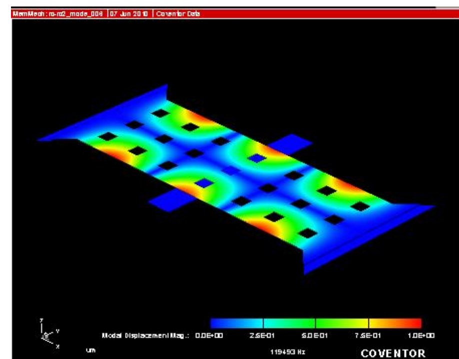

(f)

Figure 3

Harmonic analysis of design-1 switch (a) - (f) shows the six modes from 1 to 6

3.3 Analysis of MEMS Switches-Electromagnetics Properties

The electromagnetic properties of the switches are calculated by using HFSS software. The switches are simulated in both down and up states, fig. 5 and 6 shows the S-parameters results i.e. insertion, return loss and isolation of all designed switches.

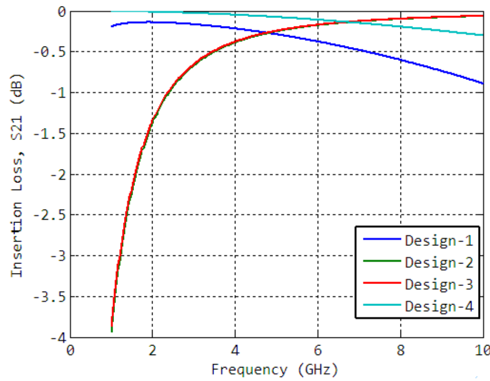

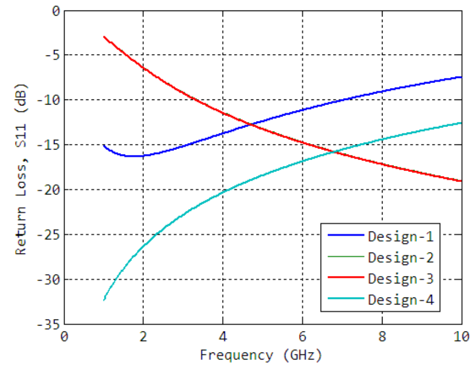

(a) (b)

Figure 5

Simulated S-parameter of Designed switches (a) insertion loss and (b) Return loss in on-state.

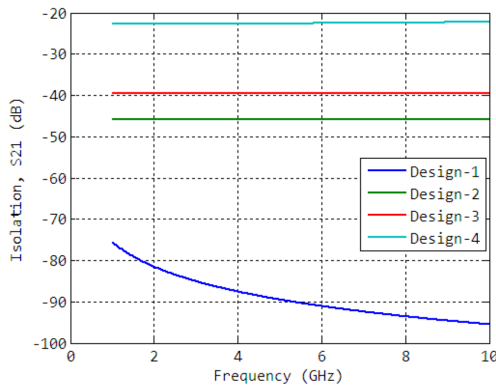

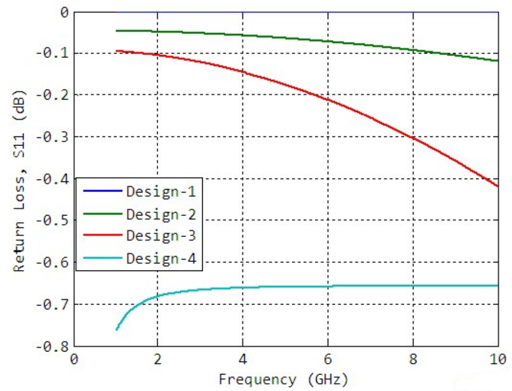

(a) (b)

Figure 6

Simulated S-parameter of Designed switches (a) Isolation loss and (b) Return loss in off-state.

4 Comparison among RF MEMS Switches

The above version of four proposed switches are chosen for comparison since all the switches has shunt configuration, almost similar dimensions and they are simulated for the study of their electromagnetic as well electromechanical characteristics, while the difference among them in beams structures are considered. Typical dimensions of all designed switch beam lengths are ranging from 250 to 400 µm and thickness ranging from 0.5 to 1.5 µm. The “Design-3”

switch show a significant improvement over the rest of three designed switches in defined operational band i.e. 1 to 8 GHz. So, its performance comparison is attempted at beginning with others in terms of electromechanical and electromagnetic properties as shown in Table 9.

Due to ease of fabrication, the “design-1” is best suited. As the shape of the beam in particular structure is “fixed-fixed” type it has relatively higher spring constant as compared with other structures. Small diameter holes of 5μm are introduced on beam which lower the mass, release some amount of resuidal stress and reduce Young’s modulus [1]. The pull-in voltage calculated in this manner is lies between 3.15 to 3.5 V. The lower mass turn yields a upper resonant frequency which is shown in generated harmonic modes (as in Fig. 3).

The serpentine spring shaped beam is considered in rest of the designs. Such variations in beams can be used to down effective value of spring constant in RF switch. The constructional difference between “Design-2” and “Design-3” are that in latter structure holes of 5 μm diameter are introduced. As a result a significantly lower actuation voltage 0.5 V instead of 22.9 V in “Design-3” was measured, combined with negligible up-state capacitance. Using 3D electrostatic simulations results, it is confirmed that the area of the holes are filled by fringing fields.

In “Design-4” the actuation area is reduced as compared with second and third design. The higher conductance and the smaller contact area ensure better electromagnetic characteristics such as insertion loss and isolation in the 1 to 8 GHz operating frequency range. Further, in this article, the evaluation of the all new propsed switches can be attained via a straight comparison with the switches as presented by authors of [11-27].

A low-loss microwave capacitive shunt MEMS switch using 5 meanders serpentine spring folded suspensions is reported earlier [11] to achieve low actuation voltage of 9 V together with the large area of capacitive actuators, so that to maintain sufficient isolation measured in off-state and on-to-off ratio capacitance is 48. A low actuation voltage of 6V MEMS switch by using low spring constant folded suspension beam mechanical structure for high frequency applications has also been reported [12]. A capacitive shunt switch which consider a see-saw type movable structure to implement a shunt (capacitive) across the CPW with a gap of 10 μm among the electrodes and the movable part and further an actuation electrostatic of 80 V has been reported earlier [13]. Mingxin Song et al. [14] have showed that both the torsion deflection and ordinary bending are influenced by the relation of arm thickness and width. Lower actuation voltage of 1.5 V is achieved by using extended torsion arm size and extended driven arm size. A capacitive MEMS switches with different meander spring beams which provide low-spring constant as well as low pull-in voltage has also been reported [15]. Depending on the serpentine design, the actuation voltages were achieved from 1.9-7.0 V. A low-loss MEMS RF switch using low actuation voltage and better mechanical stability are also known [16]. The switch MEMS has an

isolation value of - 40 dB at 10 GHz and the pull-in voltage achieved is merely 3 V. Three different membrane designs using different spring constant with single-meander, two-meander and six-strip springs to reduce the effect of residual stress and pull-in voltage have been measured and compared [17]. Shunt switch is actuated by electrostatic and electromagnetic forces combination for low voltage and power application has also been reported [18]. The coupling capacitance C_{off}/C_{on} ratio is approximately 62.5, the isolation of 20.7 dB and IL of 0.85 dB is achieved at 19.5 GHz. A shunt capacitive MEMS RF switches in III–V technology have been fabricated and designed [19] using tantalum pentoxide (Ta_2O_5) and tantalum nitride (TaN) for the dielectric layers and the actuation lines, respectively. The thin metallic membrane is used for a capacitive membrane microwave switch [20]. Electromagnetic model for capacitive shunt switch for millimeter-micrometer wave applications has also been reported [21]. The IL in the up-position is corresponding to the CPW t-line loss. It is also revealed that sudden rise in the value of down position isolation is 20+ dB could be attained with the selection of the exact LC series resonant frequency of the RF switch. The equivalent LCR circuit of the shunt RF switch used in the structure of altered 2- and 4-bridge "cross" switches from 10 to 40 GHz has also been given [22]. The 300µm long gold bridge is used and the gap height reduced from 3.5 to 1.5 µm to lower the pull-in voltage from 50 to 15 V. The IL in the up-position is 0.2–0.4 dB and down- position capacitance of 2.2 pF resulted in a high value of isolation. A RF MEMS TiO_2 capacitive switch with high capacitive ratio & low-actuation voltage on high resistivity silicon (HRS) material weighted down on a semi-suspended CPW showed an attenuation of 0.1dB/mm in the t-line [23].

The development of multilayer design methods and their properties by studying the behavior of the capacitive MEMS switches at three unlike stages is pioneered by F. Giacomozzi et al. [24]. The shunt switch capacitance was 4.6 pF and by introduction of the floating metal layer the bridge realized a capacitance of near 7.7 pF, important to a Con/Coff ratio higher than 200 which is maximum around 50 times more than the ones reached for the identical designs without this feature. Capacitive switches on microwave laminate having MEMS device monolithically integrated with other elements offering adaptability and re-configurability features have also been reported [25]. The dual warped beam type switches demonstrate in [26], who showed an off-to-on capacitive ratio of up to 170, exhibiting very good RF performance. The effect of varying the different geometric physical dimensions on the S-parameters has been demonstrated by Bahmanyar et al. [27].

Conclusions

In this article, four different MEMS RF switches are designed, analyzed and compared. We have studied the relations of actuated voltage, Young's modulus, material composition, C_{on}/C_{off} and electrostatic-forces of shunt MEMS switches with the help of coventor software. Minimum pull-in voltage calculated for serpentine beam switch with hole ("Design-3") is found to be around 0.5 V. The

lower pull-in voltage is desirable in those circuits which require less power consumption like RF MEMS based mobile front-end section. The effect of various

Table 9

Comparison of various RF MEMS switch design (operating band 1 to 10 GHz)

Ref.	Pull-in voltage	Return loss in up-state (S_{11})	Insertion loss (S_{21})	Return loss in down-state (S_{11})	Isolation (S_{21})
[11]	9 V	21 dB at 10GHz	0.11dB at 10GHz	0.98dB at 10 GHz	15 dB at 10 GHz
[12]	6V	-	-	-	-
[13]	5 V	-	0.5 dB at 10 GHz	<0.5 dB at 10 GHz	28 dB at 2.3 GHz
[14]	1.5 V	-	-	-	-
[15]	1.9- 7 V	-	-	-	-
[16]	3 V	10 dB at 10 GHz	0.37 dB at 10 GHz	-	40dB at 10 GHz
[18]	3.7 V	15 dB at 10 GHz	0.3 dB at10 GHz	0.99 dB at 10 GHz	12.5dB at 10 GHz
[19]	15–20 V	10 dB at 10 GHz	0.6 dB at 10 GHz	0.4 dB at 10 GHz	12.5dB at 10 GHz
[20]	50 V	2.5 dB at 10 GHz	0.16 dB at 10 GHz	0.2 dB at 10 GHz	15 dB at 10 GHz
[21]	20-50 V	20 dB at 10 GHz	0.07–0.1 dB from 1 to 10 GHz	0.005–0.015 dB from 1 to 10 GHz	12-14 dB at 10 GHz
[22]	15 to 25 V	22 dB at 10 GHz	0.1–0.3 dB from 1 to 10 GHz	1-2 dB at 10 GHz	8 dB at 10 GHz
[23]	8 V	-	0.4 dB at 10 GHz	-	24 dB at 10 GHz
[24]	< 10 V	35 dB at 10 GHz	0.1 dB at 10 GHz	-	20 dB at 10 GHz
[25]	30-40 V	12 dB at 10 GHz	<0.4dB at 10 GHz	0.2 dB at 10 GHz	18dB at 10 GHz
[26]	27 V	-	0.2 dB at 10.5 GHz	-	41 dB at 10.5 GHz
[27]	-	-	0.65dB at 1-10 GHz	-	12dB to 38dB at 1-10 GHz
Design-1	3.19-3.5V	13.80 dB @ 4 GHz 9.09 dB @ 8 GHz	0.22 dB @ 4 GHz 0.61 dB @ 8 GHz	0.003 dB @ 4 GHz 0.003 dB @ 8 GHz	87.7 dB @ 4 GHz 73.6 dB @ 8 GHz
Design-2	22.8-23.1V	11.40 dB @ 4 GHz 17.10 dB @ 8 GHz	0.38 dB @ 4 GHz 0.10 dB @ 8 GHz	0.004 dB @ 4 GHz 0.004 dB @ 8 GHz	45.9 dB @ 4 GHz 45.8 dB @ 8 GHz
Design-3	0.51-0.52V	11.50 dB @ 4 GHz 17.20 dB @ 8 GHz	0.36 dB @ 4 GHz 0.09 dB @ 8 GHz	0.009 dB @ 4 GHz 0.009 dB @ 8 GHz	40.1 dB @ 4 GHz 40.2 dB @ 8 GHz
Design-4	0.63-0.75V	20.30 dB @ 4 GHz 14.40 dB @ 8 GHz	0.05 dB @ 4 GHz 0.19 dB @ 8 GHz	0.675 dB @ 4 GHz 0.659 dB @ 8 GHz	23.1 dB @ 4 GHz 23.4 dB @ 8 GHz

values of electrostatic force on displacement is also calculated. As electrostatic force is increased, displacement of beam decreased. Further, the effect of beam

thickness on pull-in voltage has also studied. The thickness of beam had direct relationship with pull-in voltage, i.e. as the thickness of beam increased, the pull-in voltage also increased. This article laid the foundation for proposing a new improved RF MEMS on/off switches for reconfigurable planar antenna, and that is the subject of our future work.

Acknowledgements
This work was supported by National Program on Micro and Smart Systems (NPMASS) and also MANCEF, New Mexico, USA for providing coventoreware, comsol and other useful softwares.

References

[1] G. M. Rebeiz: RF MEMS Theory, Design, and Technology, John Wiley & Sons, Inc. New Jersey, 2003

[2] C. W. Jung, M. J. Lee, G. P. Li, F. D. Flaviis: Reconfigurable Scan-Beam Single-Arm Spiral Antenna Integrated with RF-MEMS Switches, IEEE Trans. on Antennas and Propag. Vol. 54, No. 2, 2006, pp. 455-463

[3] L. Zhou: RF MEMS DC Contact Switches for Reconfigurable Antennas, M.S. thesis, San Diego State University, 2006

[4] S. Fouladi and R. R. Mansour: Capacitive RF MEMS Switches Fabricated in Standard 0.35-μm CMOS Technology, IEEE Trans. on Microw. Theory and Techniques, Vol. 58, No. 2, 2010, pp. 478-486

[5] P. Chawla and R. Khanna: A Novel Design and Optimization Approach of RF MEMS Switch for Reconfigurable Antenna Using ANN Method, in IEEE International Conference on Communications Devices and Intelligent Systems (CODIS) 2012, pp. 188-191

[6] K. Kuwabara, K. Takagahara, H. Morimura, Y. Sato: RF MEMS Switches Integrated with Sealed Suspended Coplanar Waveguides for Reconfigurable RF Circuits, IEEE Transducers, Beijing, China, 2011, pp. 5-9

[7] C. A. Balanis Antenna Theory: Analysis and Design, third edition, John Wiley & Sons, Inc.

[8] http://www.memscap.com/aboutmems.html

[9] CoventorWare, Release by CoventorWare Inc., 2010

[10] R. L. Liboff and G. C. Dalman: Transmission Lines, Waveguide and Smith Chart, New York, pp. 237-238

[11] S. Pacheco, C. T. Nguyen, and L. P. B. Katehi: Design of Low Actuation Voltage RF MEMS Switch, in IEEE MTT-S International Microwave Symposium Digest, Baltimore, 2000, pp. 165-168

[12] D. Peroulis and S. P. Pacheco: Electromechanical Considerations in Developing Low-Voltage RF MEMS Switches, IEEE Transactions on Microwave Theory and Techniques, Vol. 51, January 2003, pp. 259-270

[13] J. M. Cabral and A. S. Holmes: A Novel Seesaw-Type RF MEMS Switch, Proc. Melecon, Malaga, Spain, May 2006, pp. 288-292

[14] M. Song, J. Yin, X. He and Y. Wang: Design and Analysis of a Novel Low Actuation Voltage Capacitive RF MEMS Switches, Proceedings of the 3rd IEEE Int. Conf. on Nano/Micro Engineered and Molecular Systems January, 2008, pp. 235-238

[15] H. Jaafar, O. Sidek, A. Miskam, S. Korakkottil: Design and Simulation of Microelectromechanical System Capacitive Shunt Switches, American Journal of Engineering and Applied Sciences, Vol. 2, No. 4, 2009, pp. 655-660

[16] B. Mishra and R. Panigrahi: Highly Stabilized MEMS Switch with Low Actuation Voltage, International Journal of Recent Trends in Engineering, November, Vol. 2, No. 7, 2009, pp. 120-122

[17] J. Sharma, N. Krishanapura and A. D. Gupta: Fabrication of Low Pull-In Voltage RF MEMS Switches on Glass Substrate in Recessed CPW Configuration for V-Band Application, Journal of Micromechanics and Microengineering, IOP Publishing, Feb. 2012

[18] Il-J. Cho, T. Song and Sang-H. Baek: A Low-Voltage and Low-Power RF MEMS Series and Shunt Switches Actuated by Combination of Electromagnetic and Electrostatic Forces, IEEE Transactions on Microwave Theory and Techniques, Vol. 53, No. 7, 2005, pp. 2450-2457

[19] A. Persano, A. Cola, G. D. Angelis, A. Taurino. P. Siciliano and F. Quarant: Capacitive RF MEMS Switches with Tantalum-based Materials, Journal of MEMS, IEEE, Vol. 20, No. 2, 2011, pp. 365-370

[20] Z. J. Yao, S. Chen and S. Eshelman: Micromachined Low-Loss Microwave Switches, IEEE Journal of Microelectromechanical Systems, June 1999, Vol. 8, No. 2, 1999, pp. 129-134

[21] J. B. Muldavin and G. M. Rebeiz: High Isolation MEMS Shunt Switches; Part 1: Modeling, IEEE Trans., Microwave Theory Tech., Vol. 48, No. 6, June 2000, pp. 1045-1052

[22] J. B. Muldavin and G. M. Rebeiz: High Isolation MEMS Shunt Switches; Part 2: Design, IEEE Trans., Microwave Theory Tech., Vol. 48, No. 6, June 2000, pp. 1053 -1056

[23] M. Fernandez-Bolanos, J. Perruisseau-Carrier, P. Dainesi and A.M. Ionescu: RF MEMS Capacitive Switch on Semi-suspended CPW Using

Low-Loss High-Resistivity Silicon Substrate, Microelectronic Engineering, ScienceDirect, Vol. 85, 2008, pp. 1039-1042

[24] F. Giacomozzi, C. Calaza, S. Colpo and V. Mulloni: Development of High Con Coff Ratio RF MEMS Shunt Switches, Romanian Journal of Information Science and Technology, Vol. 11, No. 2, 2008, pp.143-151

[25] M. W. N. Silva and S. E. Barbin: Fabrication and Testing of RF-MEMS Switches Using PCB Techniques, SBMO/IEEE MTT-S International Microwave & Optoelectronics Conference 2009, pp. 96-100

[26] R. Al-Dahleh, and R. R. Mansour: High-Capacitance-Ratio Warped-Beam Capacitive MEMS Switch Designs, Journal Of Microelectromechanical Systems, 2010, Vol. 19, No. 3, June 2010, pp. 538-547

[27] P. Bahmanyar, Kh. Mafinezhad and M. Bahmanya: Switching Performance Analysis in RF MEMS Capacitive Shunt Switches by Geometric Parameters Trade-offs, IEEE APCCAS, 2010, pp. 831-834

[28] P. Chawla and R. Khanna: Optimization Algorithm of Neural Network on RF MEMS Switch for Wireless and Mobile Reconfigurable Antenna Applications, Proceedings of Second IEEE International Conference on Parallel, Distributed and Grid Computing, PDGC-2012, 06-08 December, 2012, pp. 735-740

[29] K, Van Caekenberghe: Modeling RF MEMS Devices, IEEE Microwave Magazine, 2012, Vol. 13, No. 1, pp. 83-110

[30] M. N. Spasos: RF-MEMS Switches for Reconfigurable Antennas, Brunel University School of Engineering and Design PhD Theses, 2011

[31] F. Giacomozzi, C. Calaza, S. Colpo, V. Mulloni, A. Collini, B. Margesin, P. Farinelli, F. Casini, R. Marcelli, G. Mannocchi, L. Vietzorreck: Tecnological and Design Improvements for RF MEMS Shunt Switches, in IEEE International Semiconductor Conference, 2007, pp. 263-266

[32] F. M. Guo, Z. Q. Zhu, Y. F. Long, W. M. Wang, S. Z. Zhu, Z. S. Lai, N. Li, G. Q. Yang, W. Lu: Study on Low Voltage Actuated MEMS RF Capacitive Switches, Sensors & Actuators: A. Physical, 2003, Vol. 108, No. 1-3, pp. 128-133

[33] Y. Shim, Z. Wu, M. Rais-Zadeh: A Multimetal Surface Micromachining Process for Tunable RF MEMS Passives, IEEE Journal of Microelectromechanical Systems, 2012, Vol. 21, No. 4, pp. 867-874

[34] A. K. Sahu and B. K. Sarkar: A Novel Low Actuation Voltage RF MEMS Shunt Capacitive Switch, in IEEE International conference on Applied Electromagnetics Conference (AEMC) 2009, pp. 1-3